COMMUNICATION

Morphology-Selective Formation and Morphology-Dependent Gas-Adsorption Properties of Coordination Polymer Particles

By *Hee Jung Lee, Won Cho, Soyoung Jung,* and *Moonhyun Oh**

Coordination polymers are very useful materials in catalysis, optics, recognition, and separation.[1] In particular, there is an enormous interest in the storage of gas molecules, that is, H_2, CO_2, C_2H_2, etc.[2] Although the vast majority of coordination polymer materials, including metal–organic frameworks (MOFs), are focused on macroscaled crystalline products, for structural studies based on single-crystal X-ray analysis, we and others have recently reported the synthetic strategies for the preparation of nano- and microsized coordination polymer particles (CPPs).[3,4] In contrast to bulk coordination polymers, CPPs have considerable potential for use in innovative applications, such as imaging probes and heterogeneous catalysts.[3] Furthermore, CPPs also provide the opportunity for the fine tuning of materials, to achieve the properties desired.[4a,b] On the other hand, manipulation of the chemical and physical properties of metal or semiconductor particles through morphology control is a well-known strategy.[5] However, no research related to morphology-dependent properties in CPPs has been performed. Herein, we report the selective formation of CPPs with diverse shapes from the same basic building blocks. We also demonstrate that the gas-sorption properties of CPPs, despite their identical chemical compositions, vary according to the morphology of the particles.

A carboxyl-functionalized ligand ($H_2L = $ 2,6-bis[(4-carboxy-anilino)carbonyl]pyridine, Fig. 1a) was synthesized according to the literature[6] with slight modifications. Subsequently, CPPs were prepared by the following solvothermal reactions. H_2L, $In(NO_3)_3 \cdot xH_2O$, imidazole, and CH_3CO_2H were combined in dimethylformamide (DMF), and the resulting solution was heated at 80 °C for 10 min. After this time, the precipitated products were cooled to room temperature, collected by centrifugation, and rinsed several times with DMF and methanol.

The morphology of the resulting products was characterized by field-emission scanning electron microscopy (SEM), optical microscopy (OM), and fluorescence microscopy (FM), as shown in Figure 1b. The images reveal the formation of elongated hexagonal particles (CPP-6), with an average width and length of 1.52 and 3.00 μm, respectively. Infrared spectroscopy was used to confirm the creation of coordination polymers, as evidenced by a shift in CO stretching frequency of the carboxylate group to 1605 cm^{-1}. This value can be compared to that of 1688 cm^{-1} for the uncoordinated precursor H_2L. The chemical composition of CPP-6 was determined by energy-dispersive X-ray (EDX, Supporting Information) spectroscopy and elemental analysis (EA). As shown in the inset of Figure 1b, CPP-6 is fluorescent in the blue region of the spectrum, due to ligand-to-metal charge-transfer (LMCT) of the coordination polymer.[7] In contrast, the free ligand does not emit and luminescence in this range.

SEM and OM images of products generated in the presence of 100 μL of acetonitrile under otherwise identical reaction conditions reveal the selective formation of ellipsoidal particles (CPP-7, Fig. 2a), rather than elongated hexagons (CPP-6). The ellipsoidal-shaped CPPs have an average width and length of 1.33 and 3.40 μm, respectively. By increasing the amount of acetonitrile to 200 μL, while maintaining other reaction conditions, rod-shaped particles (CPP-8) were discriminatively generated, with an average width and length of 0.62 and 4.16 μm, respectively, as characterized by SEM and OM (Fig. 2b). Interestingly, despite the variety of morphologies, all particles
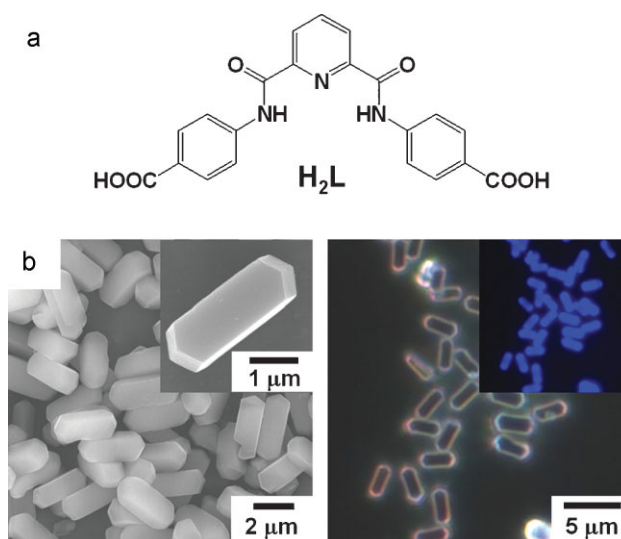

Figure 1. a) Organic precursor H_2L, used for the preparation of CPP-6, -7, and -8. b) SEM (left, inset is the high-magnification SEM image), OM (right), and FM (right inset) images of the elongated hexagons CPP-6.

[*] Prof. M. Oh, H. J. Lee, W. Cho, S. Jung
    Department of Chemistry, Yonsei University
    134 Shinchon-dong, Seodaemun-gu
    Seoul 120-749 (Korea)
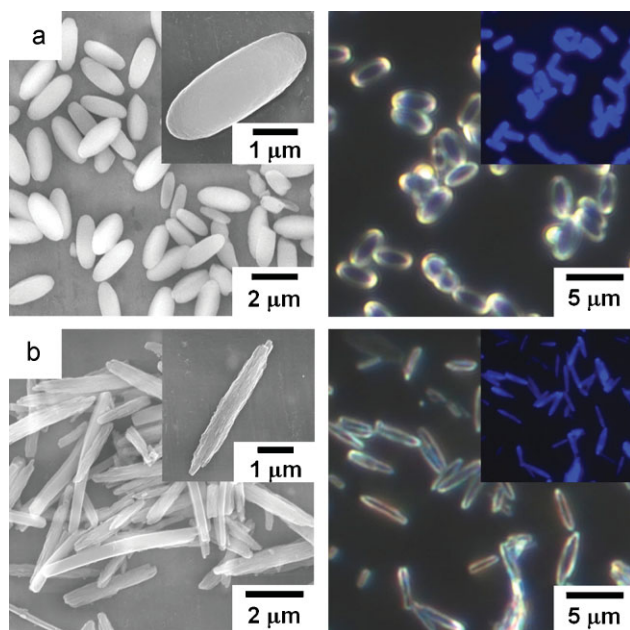   E-mail: moh@yonsei.ac.kr

Figure 2. SEM (left, inset is the high-magnification SEM image), OM (right), and FM (right inset) images of a) the ellipsoids CPP-7 and b) the rods CPP-8.
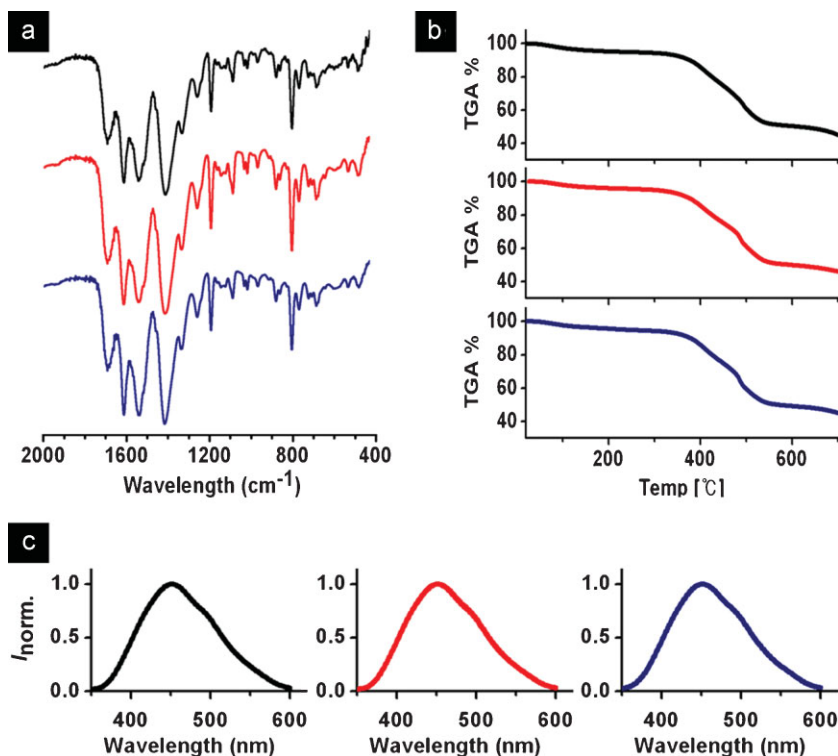

Figure 3. a) IR spectra, b) TGA results, and c) emission spectra of a series of CPP-6 (black), CPP-7 (red), and CPP-8 (blue). Data for all three CPPs are identical. Excitation wavelength = 320 nm.
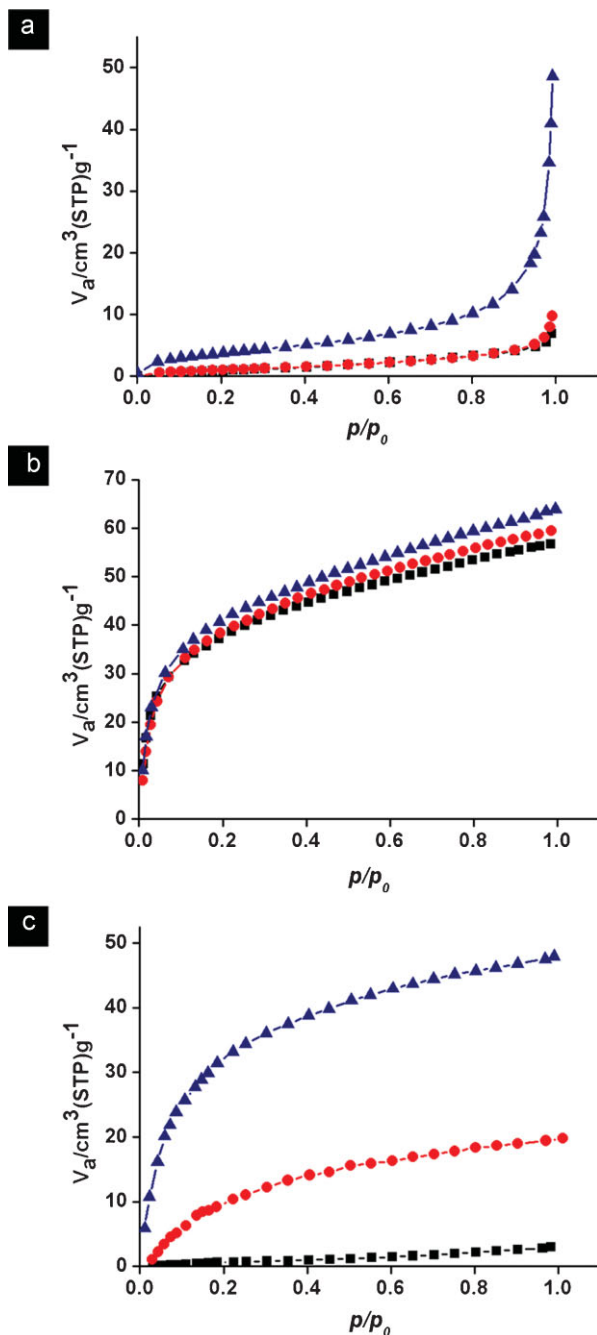
consisted of the same components, as verified by numerous experimental data (Fig. 3 and Supporting Information). First, the infrared spectra of the three CPPs are exactly identical, including the CO stretching frequency of the carboxylate group (Fig. 3a). Second, thermogravimetric analyses (TGA) of the three types of particles show the exact same profile, including first weight loss at the beginning of heating, decomposition temperature at around 370 °C, and an end-point of the rapid weight loss at around 530 °C (Fig. 3b). Third, emission spectra of the three samples overlap exactly, with the same maximum emission wavelength at 451 nm upon excitation at 320 nm (Fig. 3c). In addition to these data, EA data of the three CPPs show the same percentages on carbon, nitrogen, and hydrogen atoms, ^1H NMR spectra of the digested particles reveal that an identical portion of **L** and imidazole molecules are incorporated into all three CPPs, and XRD spectra show the same profile even though CPPs do not form perfect crystallites in dry condition (Supporting Information). All of these experimental evidences strongly support that the three CPPs generated with different shapes have the same components.[8]

Subsequently, gas-adsorption measurements for the CPPs were carried out using N_2, H_2, and CO_2. All gas-adsorption isotherms were measured after pretreatment under a dynamic vacuum at 150 °C. As shown in Figure 4a, N_2 adsorption isotherms of CPP-6, -7, and -8 exhibit the behavior for multilayer adsorption. The BET and Langmuir surface area of CPP-8, at 13.498 $m^2 g^{-1}$ and 24.804 $m^2 g^{-1}$, respectively, are larger than those of CPP-6, at 4.465 $m^2 g^{-1}$ and 10.408 $m^2 g^{-1}$, and CPP-7, at 4.492 $m^2 g^{-1}$ and 10.688 $m^2 g^{-1}$. This can be easily understood from the fact that CPP-8 has a thinner shape, and consequently more surface area than CPP-6 and CPP-7. Nonetheless, CO_2 adsorption capacities of three CPPs are significantly greater than N_2 adsorption capacities (Fig. 4b). There are several examples of this type of differential gas adsorption in coordination polymers.[9] The low N_2 adsorption is the result of strong quadrupole interactions between N_2 molecules and the electrostatic-field gradients around the surface, blocking the pore window.[9b,10] However, the relatively high thermal energy of CO_2 at 195 K makes it possible to overcome this quardrupole interaction. The specific surface area of CPP-6, deduced from the analysis of the measurements on the CO_2 adsorption at 195 K, was 196.92 $m^2 g^{-1}$. The surface areas of CPP-7 and CPP-8 based on the CO_2 adsorption are similar to that of CPP-6.

In contrast, H_2 uptake abilities of the three diversely shaped CPPs are quite different. Hydrogen-storage capacities of CPP-6, CPP-7, and CPP-8 at 77 K and under $< 1.01 \times 10^5$ Pa are 3.0095, 19.816, and 47.928 $cm^3 g^{-1}$, respectively (Fig. 4c). The reason for such different hydrogen-adsorption properties can be found in the morphology and the defects on the surface of the CPPs. First, the H_2-adsorption isotherm of CPP-6 at 77 K shows multilayer adsorption behavior, as in the case of N_2

the low solubility of CPPs, and consequently seems to result in incomplete growth/packing and so defects on the surface.

In conclusion, we have demonstrated that CPPs with three different types of morphology, namely elongated hexagons, ellipsoids, and rods, can be selectively generated from the same molecular building blocks. Notably, the diversely-shaped CPPs have different gas-adsorption properties for several gas molecules, even though they have the same components. Although the gas-storage capacities demonstrated here are not yet great, this work shows the feasibility of improving the gas-storage capacity, and possibly other properties, of coordination polymer materials by means of morphology control.

Experimental

General Methods: Solvents and all other chemicals were obtained from commercial sources and used as received unless otherwise noted. Infrared spectra of solid samples as KBr pellets were obtained using a Nicolet Avatar 360 FT-IR spectrometer. Emission spectra were obtained using a Hitachi Model F-4500 fluorometer using quartz cells (10×4 mm light path). Elemental analyses were performed at the Organic Chemistry Reaction Center, Sogang University. All SEM images and EDX spectra were obtained using either a Hitachi S-4300 field-emission SEM equipped with a Horiba EMAX 6853-H EDS system (Center for Microcrystal Assembly, Sogang University) or a JEOL JSM-6500F field-emission SEM equipped with a JEOL EX-23000 BU EDS system (Yonsei Nanomedical National Core Research Center). All optical- and fluorescence-microscopy images were obtained using a Zeiss Axio Observer.D1m optical/fluorescence microscope equipped with an AxioCam MRc 5 digital camera (Filter set 49 DAPI shift-free was used for blue emission). X-ray diffraction studies were conducted using a Rigaku D/MAX-RB equipped with a graphite-monochromated Cu Kα radiation source (40 kV, 120 mA). ^{1}H NMR and ^{13}C NMR were recorded using a Bruker advance/DPX 250 spectrometer (^{1}H NMR, 250 MHz; ^{13}C NMR, 62.5 MHz) or a Bruker advance/DRX 400 spectrometer (^{1}H NMR, 400 MHz; ^{13}C NMR, 100 MHz), with chemical shifts reported relative to residual deuterated solvent peaks. High-resolution mass spectra were recorded using a JEOL JMS AX505WA spectrometer using the fast-atom bombardment (FAB) method. TGA measurements were carried out using a Shimadzu TGA-50 in a nitrogen atmosphere at a heating rate of $5\,^{\circ}C\,min^{-1}$. The adsorption isotherms of CO_2 (195 K), N_2 (77 K), and H_2(77 K) were measured in the gaseous state using BELSORP II-mini volumetric adsorption equipment. All gas-adsorption isotherms were measured after pretreatment under a dynamic vacuum at $150\,^{\circ}C$.

Synthesis of **H₂L**: 2,6-bis[[(4-carboxyanilino)carbonyl]pyridine (**H₂L**) was synthesized according to the modified literature method [6]. Acetonitrile (25 mL) was used to dissolve 2,6-pyridinedicarbonyldichloride (4.90 mmol), and the resulting solution was added to an acetonitrile solution (25 mL) of *p*-aminobenzoic acid (10.79 mmol). The resulting mixture was refluxed for 1.5 h. The precipitated products were isolated by filtration and recrystalized in methanol (93% Yield). ^{1}H NMR (400 MHz, dimethyl sulfoxide(DMSO)-*d₆*, δ): 11.25 (s, 2H, NH), 8.44 (d, $J = 7.6$ Hz, 2H), 8.32 (t, $J = 7.6$ Hz, 1H), 8.10–8.02 (m, 8H). ^{13}C NMR (100 MHz, DMSO-*d₆*, δ): 167.06, 162.00, 148.62, 141.98, 140.18, 130.33, 126.70, 125.77, 120.17. IR (KBr): $\nu = 1688.5$ (s), 1608.1 (m), 1588.2 (m), 1529.4 (s), 1449.0 (w), 1411.5 (m), 1317.6 (m), 1289.4 (m), 1246.9 (m), 1175.7 (m), 1116.3 (m), 1077.6 (w), 1000.4 (w), 857.0 (w), 771.8 (w), 733.0 (w), 682.9 (w), 655.6 (w), 634.9 (w), 549.3 (w), 506.7 cm^{-1} (w). HRMS (FAB, *m/z*): [M] calcd for $C_{21}H_{15}N_3O_6$, 405.0961; found, 405.0962. Anal. calcd for **H₂L**, $C_{21}H_{15}N_3O_6$: C 62.22, H 3.73, N 10.37; found: C 62.29, H 3.61, N 10.16.

Preparation of CPP-6: A precursor solution was prepared by mixing **H₂L** (3.00 mg, 0.0074 mmol) and $In(NO_3)_3 \cdot xH_2O$ (6.36 mg, 0.016 mmol) in 0.8 mL DMF in the presence of imidazole (0.032 mmol) and acetic acid (0.022 mmol). The resulting mixture was placed in an oil bath ($80\,^{\circ}C$). After

Figure 4. Gas-adsorption isotherms for a) N_2 on adsorbents at 77 K, b) CO_2 on adsorbents at 195 K, and c) H_2 on adsorbents at 77 K of a series of CPP-6 (black square), CPP-7 (red circle), and CPP-8 (blue triangle).

adsorption. However, CPP-7 has some surface defects, resulting in the rather bigger pore windows on the rough surface (Fig. S5), where hydrogen molecules can access the interior of the particles. Note that the kinetic diameter of H_2 (2.8 Å) is smaller than that of N_2 (3.6 Å).[11] CPP-8 has many more surface defects (Fig. S6), which will give rise to additional big-enough pore windows for H_2 molecules to pass. The presence of acetonitrile during the synthesis of CPP-7 and CPP-8 induces rapid precipitation, due to

10 min, the elongated hexagonal particles (CPP-6) were formed. Products generated were cooled to room temperature, isolated, and subsequently washed with DMF and methanol several times, via centrifugation–redispersion cycles. Each successive supernatant was decanted and replaced with fresh DMF and methanol (37% yield). IR (KBr): $\nu = 1685.6$ (s), 1604.8 (s), 1533.6 (s), 1400.6 (s), 1321.5 (w), 1246.2 (w), 1178.5 (s), 1125.1 (w), 1071.9 (w), 1000.9 (w), 951.2 (w), 859.1 (w), 782.1 (s), 747.6 (w), 701.3 (w), 662.9 (w), 507.8 (w), 459.6 cm^{-1} (w). Anal. calcd for CPP-6, $C_{45}H_{36}In_2N_8O_{16}$: C 46.02, H 3.09, N 9.54; found: C 46.09, H 3.12, N 9.55.

Preparation of CPP-7: The ellipsoidal particles (CPP-7) were prepared in the presence of 100 μL acetonitrile under otherwise identical reaction conditions to those described above (51% yield). IR (KBr): $\nu = 1685.7$ (s), 1605.4 (s), 1533.2 (s), 1402.7 (s), 1246.2 (w), 1178.9 (s), 1128.7 (w), 1071.8 (w), 1000.5 (w), 950.5 (w), 859.9 (w), 782.6 (s), 747.8 (w), 701.0 (w), 663.4 (w), 507.7 (w), 457.6 cm^{-1} (w). Anal. calcd for CPP-7, $C_{45}H_{36}In_2N_8O_{16}$: C 46.02, H 3.09, N 9.54; found: C 46.03, H 3.02, N 9.63.

Preparation of CPP-8: The rod-shaped particles (CPP-8) were prepared in the presence of 200 μL acetonitrile under otherwise identical reaction conditions to those described above (42% yield). IR (KBr): $\nu = 1685.6$ (s), 1605.0 (s), 1529.5 (s), 1405.9 (s), 1324.3 (w), 1246.5 (w), 1178.7 (s), 1129.7 (w), 1072.6 (w), 1000.3 (w), 949.4 (w), 860.1 (w), 782.8 (s), 747.8 (w), 700.9 (w), 663.1 (w), 507.3 (w), 455.0 cm^{-1} (w). Anal. calcd for CPP-8, $C_{45}H_{36}In_2N_8O_{16}$: C 46.02, H 3.09, N 9.54; found: C 45.99, H 2.98, N 9.59.

Acknowledgements

[1] a) O. R. Evans, W. Lin, *Acc. Chem. Res.* **2002**, *35*, 511. b) J. S. Seo, J. Whang, H. Lee, S. I. Jun, J. Oh, Y. J. Jeon, K. Kim, *Nature* **2000**, *404*, 982. c) F. M. Tabellion, S. R. Seidel, A. M. Arif, P. J. Stang, *J. Am. Chem. Soc.* **2001**, *123*, 7740. d) B. Chen, L. Wang, F. Zapata, G. Qian, E. B. Lobkovsky, *J. Am. Chem. Soc.* **2008**, *130*, 6718. e) S. Hasegawa, S. Horike, R. Matsuda, S. Furukawa, K. Mochizuki, Y. Kinoshita, S. Kitagawa, *J. Am. Chem. Soc.* **2007**, *129*, 2607. f) S. Horike, M. Dincǎ, K. Tamaki, J. R. Long, *J. Am. Chem. Soc.* **2008**, *130*, 5854. g) S.-N. Wang, Y. Yang, J. Bai, Y.-Z. Li, M. Scheer, Y. Pan, X.-Z. You, *Chem. Commun.* **2007**, 4416.

[2] a) O. M. Yaghi, M. O'Keeffe, N. W. Ockwig, H. K. Chae, M. Eddaoudi, J. Kim, *Nature* **2003**, *423*, 705. b) R. Matsuda, R. Kitaura, S. Kitagawa, Y. Kubota, R. V. Belosludov, T. C. Kobayashi, H. Sakamoto, T. Chiba, M. Takata, Y. Kawazoe, Y. Mita, *Nature* **2005**, *436*, 238. c) K. L. Mulfort, J. T. Hupp, *J. Am. Chem. Soc.* **2007**, *129*, 9604. d) R. Banerjee, A. Phan, B. Wang, C. Knobler, H. Furukawa, M. O'Keeffe, O. M. Yaghi, *Science* **2008**, *319*, 939.

[3] a) W. J. Rieter, K. M. L. Taylor, H. An, W. Lin, W. Lin, *J. Am. Chem. Soc.* **2006**, *128*, 9024. b) K. H. Park, K. Jang, S. U. Son, D. A. Sweigart, *J. Am. Chem. Soc.* **2006**, *128*, 8740.

[4] a) M. Oh, C. A. Mirkin, *Nature* **2005**, *438*, 651. b) M. Oh, C. A. Mirkin, *Angew. Chem. Int. Ed.* **2006**, *45*, 5492. c) S. Jung, M. Oh, *Angew. Chem. Int. Ed.* **2008**, *47*, 2049. d) X. Sun, S. Dong, E. Wang, *J. Am. Chem. Soc.* **2005**, *127*, 13102. e) Y.-M. Jeon, J. Heo, C. A. Mirkin, *J. Am. Chem. Soc.* **2007**, *129*, 7480. f) Z. Shen, G. Zhang, H. Zhou, P. Sun, B. Li, D. Ding, T. Chen, *Adv. Mater.* **2008**, *20*, 984.

[5] a) S. Sun, C. B. Murray, D. Weller, L. Folks, A. Moser, *Science* **2000**, *287*, 1989. b) T. Mokari, M. Zhang, P. Yang, *J. Am. Chem. Soc.* **2007**, *129*, 9864. c) J. Chen, T. Herricks, Y. Xia, *Angew. Chem. Int. Ed.* **2005**, *44*, 2589.

[6] J. F. Malone, C. M. Murray, G. M. Dolan, R. Docherty, A. J. Lavery, *Chem. Mater.* **1997**, *9*, 2983.

[7] a) J.-C. Dai, X.-T. Wu, Z.-Y. Fu, C.-P. Cui, S.-M. Hu, W.-X. Du, L.-M. Wu, H.-H. Zhang, R.-Q. Sun, *Inorg. Chem.* **2002**, *41*, 1391. b) J. Tao, J.-X. Shi, M.-L. Tong, X.-X. Zhang, X.-M. Chen, *Inorg. Chem.* **2001**, *40*, 6328.

[8] There are inherent difficulties in determining the exact structure of CPPs, due to the limitations of X-ray diffraction. However, the molecular formula of CPPs $\{[In(L)(OH)(H_2O)] \cdot 1/2(imidazole)\}_n$ was deduced from the analysis of ^1H NMR spectra of the digested particles. And this result is consistent with EA data.

[9] a) T. K. Maji, R. Matsuda, S. Kitagawa, *Nat. Mater.* **2007**, *6*, 142. b) K. M. Ok, J. Sung, G. Hu, R. M. J. Jacobs, D. O'Hare, *J. Am. Chem. Soc.* **2008**, *130*, 3762. c) D. N. Dybtsev, H. Chun, S. H. Yoon, D. Kim, K. Kim, *J. Am. Chem. Soc.* **2004**, *126*, 32.

[10] W. Steele, *Chem. Rev.* **1993**, *93*, 2355.

[11] D. W. Beck, *Zeolite Molecular Sieves*, Wiley, New York **1974**.